Desalination and Water Treatment
www.deswater.com
doi: 10.1080/19443994.2013.770117

51 (2013) 4435–4446
June

Taylor & Francis
Taylor & Francis Group

Mathematical model for the removal of trace metal by complexation-ultrafiltration

Payel Sarkar*, S. Prabhakar, D. Goswami, P.K. Tewari

Desalination Division, Bhabha Atomic Research Centre, Mumbai 400085, India
Tel. 022 2559 4729; email: payelb@barc.gov.in

Received 8 May 2012; Accepted 16 November 2012

ABSTRACT

Complexation-ultrafiltration is emerging as the potential method for the removal of dissolved trace contaminant species from water in an energy efficient manner. The study incorporates the pore-size distribution of the membrane and the molecular weight distribution of the complexing ligand into the irreversible thermodynamic model by modifying the coefficients σ and ω to predict the rejection behavior of trace elements in the presence of complexing ligand necessitated due to the fact that the rejection behavior at trace concentrations is more dependent on probability with reference to a particular pore (related to pore diameter) and the size of the complexed species (mw of the particular species). A set of transport equations have been derived from Kedem Katachalsky's irreversible thermodynamic model, by incorporating pore-size distribution of the membrane and molecular weight distribution (derived from size distribution) of ligand (polyethyleneimine). The validation of model has been done through the experimental data with copper–polyethyleneimine system using commercially available 6, 20, and 100 KD molecular wt. cutoff hollow fiber ultrafiltration membrane in-bench scale systems. The model developed is in good agreement with the experimental results as long as the stoichiometric concentration of ligand is equal or excess compared with the heavy metal species. Further, the studies also have underlined the importance of considering the pore-size distribution for predicting the performance characteristics. The model was not found suitable when the metal species is in excess, a situation we may not normally encounter in the removal trace metal species.

Keywords: Complexation ultrafiltration; Trace metal removal; Pore-size distribution; Mathematical model; Molecular weight distribution of ligand

1. Introduction

In view of the stringent environmental standards and increasing realization that "waste is wealth," efforts are directed toward recovering trace constituents from effluent streams or from seawater. Sorption techniques are being widely investigated for preferential separation of the trace constituents such as uranium [1]. However, the presence of bulk constituents makes the process cumbersome and more often economically unviable. In the last few years, membrane based processes such as liquid membranes, ultra-fitration, nano-filtration, and reverse osmosis are emerging as alternative options for the separation or removal trace contaminants. Liquid membranes [2] can be

*Corresponding author.

highly specific but require the use of costly solvents. Nano-filtration and reverse osmosis are pressure-driven processes requiring more energy. Besides, the trace metal concentrations, which are normally in the range of a few ppb to ppm, are not well rejected as the rejection behavior is concentration-dependent (solution controlled). Even if they are rejected the separation of the species from the bulk constituents becomes difficult. Complexation-ultrafiltration operates under very low pressures and separates the complexed species from the remaining bulk species [3–11]. In most cases, complexation-ultrafiltration affords the option of recovering the metal species and ligand by changing the solution properties such as pH [5]. In complexation-ultrafiltration, the size of the trace metal species is enhanced specifically to facilitate the separation. Extensive studies have been reported in this context with respect to experimental investigations and development of mathematical models to explain the behavioral characteristics of metal ions in the presence of complexing ligands. Most of these studies aim at establishing the mechanism of separation and were carried out under laboratory conditions in flat sheets with membrane areas of about a few square centimeters. No doubt, these studies are useful in developing the basic equations for the designing or modeling but cannot be applied directly for larger systems in practice without modifying some of the assumptions and consequently effecting changes in the model equations. Some of the models proposed in the literature include assumptions such as "total rejection of the ligands through UF membranes," [3] the applicability of average experimental rejection data of pure ligand and pure metal for ligand-metal-mixed systems [10,11], etc. The membrane systems are modular in nature and the capacity can be enhanced by multiplying the unit systems. The basic unit of UF is mostly hollow-fiber-based (spiral and flat sheet configurations are also available) and is available with a large spectrum of porosity (designated in terms of molecular weight cutoff). Even though they are designated by distinct MWCOs such as 6, 20, 100 KD etc., the membranes do have a pore-size distribution which can be theoretically estimated [12–14] or determined using different species of known molecular sizes [12]. Commercially available polymeric ligands also have molecular weight distribution. Complexation is an equilibrium phenomenon and consequently free ions, free ligands, and complexed species would coexist in the feed stream. Some of these factors, which can be ignored under test cell conditions, have significant influence on the performance of the system at bench-/pilot-scale environment. Thus, there is a need to accommodate these factors in the mathematical model to facilitate application of the complexation-ultrafiltration in practice. With this objective, we have carried out experiments with Cu–Polyethylene imines (PEI) systems using commercially available UF module elements. A mathematical model has been developed by suitably incorporating the necessary corrective terms to account for the membrane and ligand characteristics. The validity of the model is examined based on the experimental results.

2. Theoretical considerations

2.1. Background

All membranes prepared by phase inversion technique have a pore-size distribution and the rejection behavior of the membrane at very low concentrations of solute species in the feed streams is governed by least resistant route for the solute passage. In practice, as the solute concentration increases from the base level of zero concentration, the solute rejection slowly increases up to a point beyond which there is a marginal decrease.

In complexation-ultrafiltration, it is presumed that the trace metal species is bound to the polymeric ligand and hence gets excluded because of the increased size. Once the complexing polymeric ligand is added to the solution containing the trace metal ions, it is expected that some metal ions would be complexed. The extent of complexation would depend on the equilibrium conditions, which in turn would be a function of pH, temperature, and relative concentration ratio of metal ion and complexing ligand. Unless the modified size is higher than all the pores present in the membrane surface, there is a probability that the modified-metal species may not be completely rejected by the membrane. The selection of the polymer with appropriate molecular weight, ratio of the polymer/metal species and the MWCO of the membrane are important to ensure efficient separation of the desired species.

Several models have been reported with different assumptions depending on the experimental systems. [3] has developed a mathematical model for measurement of binding constants of polyethyleneimine with metal ions and metal chelates in aqueous media by ultrafiltration. The model has determined the binding properties of metal ions and polymeric ligands on the assumption of total rejection of ligands. [11] evaluated the affinity of partially ethoxylated polyethyleneimine toward industrially valuable metal ions (Cu^{+2}, Ni^{+2}, Cd^{+2}, and Zn^{+2}) and proposed a model based on the competitive reaction between polymer functional groups and the cations present in the solution to predict metal rejection coefficients using the complex formation constant data. In this work, the rejection

behavior of metal and ligand have been predicted by incorporating membrane discretized pore-size distribution and ligand size distribution in an irreversible thermodynamic transport model by modifying the "reflection coefficient" and "solute permeability constant" to predict the performance.

2.2. Development of model equations

2.2.1. Complexation model

This model assumes that the equilibrium is instantaneously attained, no pH change due to the metal–ligand complex formation, no hydroxide formation, and metal–ligand formation will be governed by stoichiometries from 1:1 to 1: n [11].

Competitive reactions between metal ions (Me), ligand ions (L), and protons (H^+) have been considered as follows.

$$HL \leftrightarrow H + L;\ K_a = \frac{[H]\times[L]_{free}}{[HL]} \tag{1}$$

$$Me + nL \leftrightarrow [MeL_n]K_n = \frac{[MeL_n]}{[Me]_{free} \times [L]^n_{free}} \tag{2}$$

Mass balance applied on total concentration of metal ion

$$[Me] = [Me]_{free} + \sum_n [MeL_n] \tag{3}$$

Mass balance applied on total concentration of ligand ion

$$[L] = [L]_{free} + \frac{[L]_{free}\times[H]}{K_a} + \sum_n n \times K_n [Me]_{free} \times [L]^n_{free} \tag{4}$$

inserting the values of Eqs. (2) and (3), we get

$$[Me]_{free} = \frac{[Me]}{1 + \sum_n K^*_n [L]^n_{free}} \tag{5}$$

Inserting the expression of Eq. (5) into Eq. (4), we get

$$[L] = [L]_{free} + \frac{[L]_{free}\times[H]}{K_a} + \frac{[Me]\times\sum_n n\times K_n \times [L]^n_{free}}{1 + \sum_n K_n \times [L]^n_{free}} \tag{6}$$

Free ligand concentration is obtained by solving Eq. (6), while free metal concentration can be found out by solving Eq. (5).

Rejection of metal is given by

$$R_{Me} = \frac{R_{Mefree} + R_L \sum_n K_n \times [L]^n_{free}}{1 + \sum_n K_n \times [L]^n_{free}} \tag{7}$$

Several authors have predicted rejection of metal R_{Me} (rejection of metal in complexed form) by taking R_{Mefree} (pure-metal rejection) value and R_L (pure-ligand rejection) values from ultrafiltration experimental data [11]. Some authors have also taken R_{Mefree} value zero and R_L value 100% for mathematical simplicity[3]. In reality, R_{Mefree} is not zero for most of the UF membranes. Hence, for the model development, we have modified the terms R_{Mefree} and R_L by incorporation of discretized pore-size distribution of membranes and ligand-size distribution in Kedem–Katalaschky's transport model.

2.3. Modifications carried out in current studies

Various models based on different approaches are reported in the literature [15–17] to describe and predict the solute passage through the membrane. Kedem–Katchalsky's irreversible thermodynamics approach has been considered in this study as the molecular mechanisms of transport processes within the membrane are not fully understood. The basic equations for the solute flux and the solvent flux [17] are given as

$$J_v = L_P(\Delta p - \sigma\Delta\pi) \tag{8}$$

$$J_s = (C_s)_{ln}(1-\sigma)J_v + \omega\Delta\pi \tag{9}$$

$$(C_s)_{ln} = \frac{C_m - C_p}{\ln\frac{C_m}{C_p}} \tag{10}$$

Here, $J_{v,}$ J_s, represent solvent and solute fluxes, L_P is the filtration coefficient, ΔP is pressure drop across the membrane, σ is reflection coefficient, ω is the solute permeability, and $\Delta\pi$ is the osmotic pressure difference between the fluid on membrane surface and product stream, (C_s) is logarithmic concentration, C_m is the concentration of the solute on the membrane surface, and C_P is the concentration of the solute in the product stream.

In essence, σ indicates the solute rejection property of the membrane and ω indicates the solute permeability through the membrane. Since σ is dependent on membrane, there is a need to have an appropriate correction factor for σ, reflecting the membrane nature. Similarly, ω requires modification as it refers to

the permeability of solute species having a size distribution.

2.3.1. Incorporation of pore theory in rejection model

Pappenheimer [18], Verinory [19] incorporated pore theory for transcapillary transport. According to this theory, the membrane structure can be estimated by the parameters σ and ω. Nakao-Kimura et al. [20] has described the structural implications of the ultrafiltration membrane using this "pore theory." They have assumed that cylindrical membrane pore has a constant radius r_p and length ΔX and that the spherical solutes have a radius r_s.

σ and ω can be written in terms of pore theory as

$$\sigma = 1 - g(q) \times S_F \tag{11}$$

$$\omega = D \times f(q) \times S_D \times \left(\frac{A_k}{\Delta X}\right) \tag{12}$$

D is the diffusivity of solute. A_k is the ratio of total cross sectional pore area to the effective membrane area.

$$q = \frac{r_s}{r_p} \tag{13}$$

S_D and S_F are the steric hindrance factors for diffusion and filtration flow, respectively, and are defined as

$$S_D = (1-q)^2 \tag{14}$$

$$S_F = 2(1-q)^2 - (1-q)^4 \tag{15}$$

$f(q)$ and $g(q)$ are the correction factors for the effects of a cylinder wall and are calculated as

$$f(q) = \left(1 - 2.1q + 2.1q^3 - 1.7q^5 + 0.73q^6\right)/(1 - 0.76q^5) \tag{16}$$

$$g(q) = \left(1 - 0.6667q^2 - 0.2q^5\right)/\left(1 - 0.76q^5\right) \tag{17}$$

Eq. (9) can be rewritten

$$J_s = (C_s)_{ln}(1-\sigma)(L_p(\Delta P - \sigma\Delta\pi)) + \omega\Delta\pi \tag{18}$$

$$J_s = (C_s)_{ln}(g(q) \times S_F)(L_p(\Delta P - (1 - g(q) \times S_F)\Delta\pi)) + D \times f(q) \times S_D\frac{A_k}{\Delta X}\Delta\pi \tag{19}$$

$$J_v(C_s)_{ln} = J_s C_{water} \tag{20}$$

$$\text{Rejection} = \frac{C_m - C_P}{C_m} \tag{21}$$

$$J_w = L_p \times \Delta P = \left(\frac{r_p^2}{8\mu}\right)\left(\frac{A_k}{\Delta X}\right) \times \Delta P \tag{22}$$

$$\frac{A_k}{\Delta X} = \frac{L_p \times 8\mu}{r_p^2} \tag{23}$$

A_k is constant for a specific membrane and can be expressed in terms of pure-water flux using Hagen–Poiseuille equation Eq. (22) and J_w is pure-water permeability, μ is solvent viscosity. J_s is the solute flux (free metal as well as free ligand) L_P, C_M, and ΔP were measured during the experiments. r_p was estimated based on experimental studies. Solute fluxes for free metal, and free ligand were calculated using Eq. (19) ΔP is taken as the operating pressure as the pressure drop along the length of the membrane is negligible. As the experiments were conducted at very low concentrations, $\Delta\pi$ is not significant. However, the values could be estimated based on the molar concentrations. D, μ and r_s were obtained from the literature.

2.3.2. Estimation of mean pore diameter r_p of membranes:

UF membranes are normally characterized by taking different molecular weight of polyethylene glycol (PEG) and polyethylene oxide (PEO). The stokes radii of these species are calculated using the Eq. (22) for PEG and (23) for PEO [12,13].

$$A = 16.73 \times 10^{-10} M^{0.557} \tag{24}$$

$$A = 10.44 \times 10^{-10} M^{0.587} \tag{25}$$

where A is Stoke radius of solute in cm, M is molecular wt. in g/mol.

Following Singh et al. [12] and Michaelis et al. [13], the pore-size distribution is estimated as described; A plot of experimental values of solute rejection (%) of UF membrane against the solute diameter (as estimated from the Stokes radius) yields a straight line on a log normal probability scale. The solute diameter corresponding to 50% solute rejection is taken as the mean pore diameter of membrane (r_p). The geometric standard deviation is obtained by the ratio of solute diameters corresponding to 83.14 and 50% solute rejection, with the assumption that there

exist no steric or hydrodynamic interactions. The mean pore size μ_p and the geometric standard deviation σp of the membrane can be considered to be the same as the solute mean size and solute geometric standard deviation. From these two data points, the pore-size distribution of a ultrafiltration membrane can be expressed by the following probability density function

$$\frac{df(d_p)}{dd_p} = \frac{1}{d_p \ln \sigma_p \sqrt{2\pi}} \exp\left[-\frac{(\ln d_p - \ln \mu_p)^2}{2(\ln \sigma_p)^2}\right] \quad (26)$$

From mean pore-size data and the geometric standard deviation data, cumulative distribution function of membrane pore sizes can be obtained by MATLAB software.

2.3.3. Estimation of solute diameter (D_s)

Solute diameter of copper and polyethyleneimine were estimated using Stoke–Einstein formula Eq. (27) Where M_w is the average molecular wt. (g/mol), $[\eta]$is specific viscosity (cc/g), N_A is the Avogadro's Number.

$$D_S = 2 \times 10^{10} \left(\frac{3 \times 10^{-3} M_w [\eta]}{10\pi N_A}\right)^{1/3} \quad (27)$$

3. Materials and methods

3.1. Membrane

Hollow fiber ultrafiltration membranes supplied by Davey Product having MWCO 6, 20, and 100 KD have been used in experiments. All the membranes have been characterized by standard PEG and PEO method [12]. Mean pore size r_p of membranes have been obtained by the method described earlier. Dimensions of the membrane elements used are given in Table 1.

3.2. Pump

Horizontal centrifugal pump (CNP make, model CHL2–40) rated at 33 lpm flow 3 bar pressure was used. The feed flow 35 lpm at 2.2 bar pressure was maintained throughout the experiments by suitably manipulating the valves (concentrate recycle). The fluctuations in flow measurements were about ± 0.25 lpm and that of pressure was about ± 0.5 bar.

Table 1
Dimensions of the spiral membrane elements used for experimental studies

(KD)	Dimension (dia × width) in meters	Available area in sq m
6	0.09 × 1.1	2.8
20	0.09 × 1.1	2.8
100	0.09 × 1.1	7

3.3. Preparation of test solutions

Polyethyleneimine (Ave.MW 50 KD, AR grade) was purchased from Sigma Aldrich. Copper nitrate (AR grade) was purchased from S.D. Chemicals. All solutions were prepared in RO-treated service water, pH of solutions were adjusted by sodium hydroxide and hydrochloric acid as required.

3.4. Analysis of samples

For Copper, the samples are analyzed with atomic absorption spectroscopy (model number ICE3000 (make: Thermoscientific). Polyethyleneimine samples were analyzed with TOC (model number AnaTOC-2 SGE Australia).

3.5. Experimental system

The data for validation of the model was carried out using the experimental system as shown in Fig. 1. The feed solutions corresponding to various experimental plans were prepared in UF feed water tank. The feed is pumped through UF module and samples were drawn for analysis as per the experimental plan. To maintain the constant concentration in feed tank, both the reject and product streams were recycled back to feed tank. All set of experiments were carried out at ambient temperature slightly below neutral pH by careful addition of HCl and ensuring that no turbidity is seen indicating the absence of hydroxide formation. The experiments

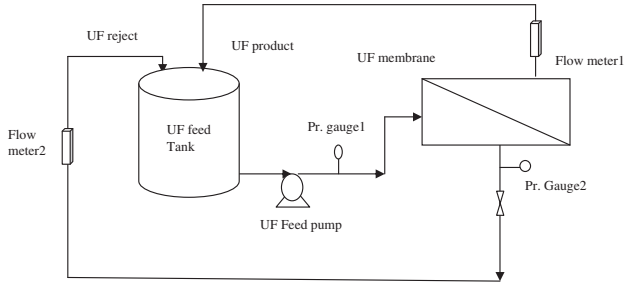

Fig. 1. Schematic diagram of Ultrafiltration complexation System.

were repeated for different UF elements. Solutions corresponding to different load factors were prepared by keeping the concentration of PEI constant at 160 ppm and varying the copper concentration.

In the original feed, the PEI concentration was 160 ppm (prepared by dissolving 8 gms in 50 l of RO-treated service water. Copper concentration was varied from 1.6 ppm to 160 ppm using copper nitrate trihydrate, Mol.wt. 241.54; for preparing 1.6 ppm copper solution, 0.304 gm copper nitrate was added in 50 l of water and for 160 ppm copper solution, 30.4 gm copper nitrate was added in 50 l of water (0.025 to 2.5 mM).

4. Results and discussion

4.1. Basic membrane and ligand characteristics

Pure water permeability (PWP) values of all the membranes as shown in Fig. 2 were experimentally measured at different operating pressures using RO permeate as feed. Membrane permeability constant (L_p) values were estimated for all the membranes from the slope of the graph corresponding to each membrane. Although there is no significant pressure drop during the experiment, in general, after every experiment, the flushing has been done for 2 min and after 2 sets of experiments backwashing was done for 30 s. Pressure drop is measured by the difference of two calibrated pressure gauge readings installed at the entry and exit points of the test module element. The feed did not contain any significant concentration of scaling components, and hence, pressure drop due to scaling was ruled out. The other possibility was fouling of the membranes due to deposition or concentration of PEI molecules near the membrane surface. As per our observations, the pressure drop was negligible (<0.2 bar, i.e. detectable limit) indicating that pressure drop due the hydrodynamics is not significant with reference to the present experimental system.

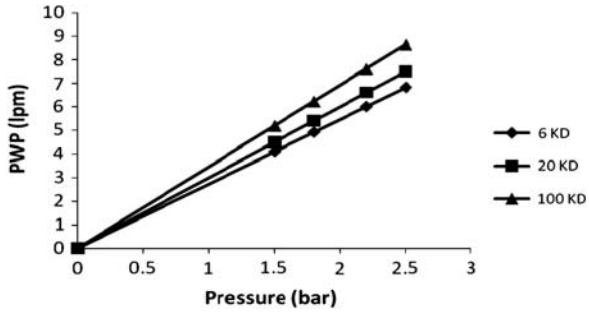

Fig. 2. Pure water permeability (PWP)s of different molecular wt. cutoff membrane.

4.2. Determination of the pore-size distribution of membrane

Following the method described in Section 2.3.2, the experimental values of solute rejection for all the three membranes were plotted in log-normal scale as shown in Fig. 3. The solute sizes corresponding to 50 and 83.14% were interpolated from the trendline and mean pore size and standard deviations were calculated as shown in Table 2.

4.3. Discretization of the pore sizes

Cumulative pore-size distribution of three different molecular wt. cutoff membranes has been calculated using MATLAB software on the basis of mean and standard deviation using Eq. (26). The cumulative pore-size distribution thus obtained as shown in Fig. 4.

For the sake of calculations, the whole domain has been arbitrarily subdivided (discretized) into ten equal subdomains and the maximum size of pore in each subdomain has been identified and the results are shown in Table 3.

4.4. Molecular weight distribution of ligands

Solute size of polyethylene-imine evaluated from Stoke Einstein Equation is 39 nm with assumed molecular weight of 50 KD. Size distribution of polyethylene-imine has been obtained from Dynamic Light Scattering (DLS). The instrument through its inbuilt

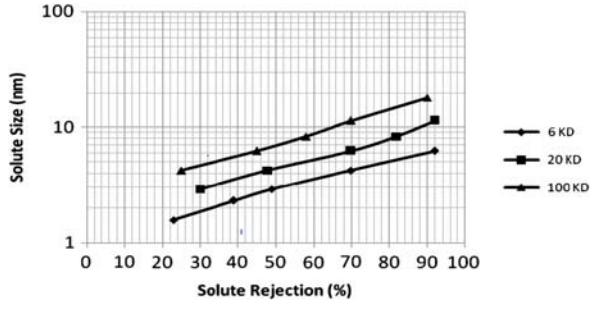

Fig. 3. Experimental values of mean solute size (nm) vs solute rejection (%).

Table 2
Mean pore size and standard deviation of the membranes

Membrane	6 KD	20 KD	100 KD
Mean pore size (nm)	3.1	4.49	7.20
Standard deviation (σp)	1.82	2.02	2.47

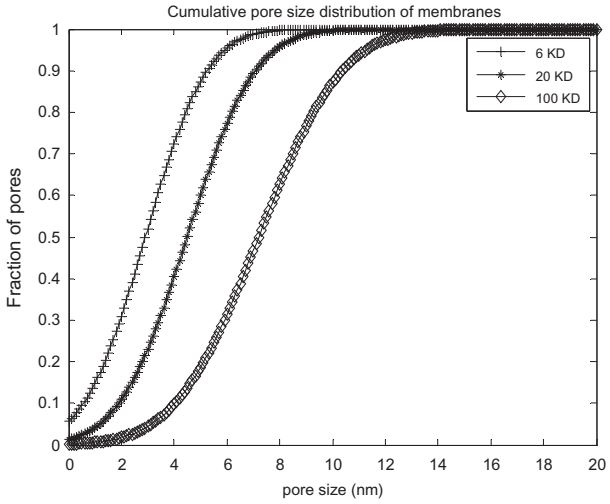

Fig. 4. Cumulative pore-size distribution.

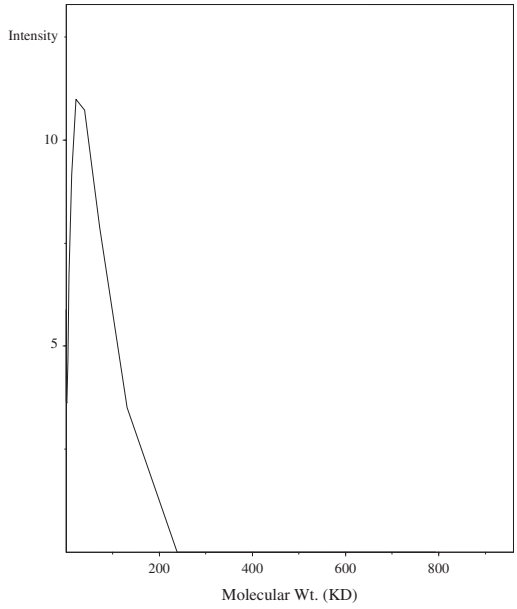

Fig. 5. Molecular wt. distribution of PEI.

software provides the size distribution and molecular weight distribution of given polymer and also the size versus weight fraction and number fraction data.

Fig. 4 provides the intensity (arbitrary units) versus molecular weight in KD and Fig. 5 provides the plot of intensity versus molecular weight and intensity versus size in nm respectively. The size distribution of polyethylene-imine along with the weight fraction of each range (represented by maximum size) derived there from through the in built software is given in Table 4. For all our studies, we have used the size distribution as given the table.

4.5. Performance of membranes in the experimental system

The solute rejection characteristics of pure copper and pure PEI at 64 and 160 ppm are shown in Fig. 7. As expected, the solute rejection decreases with increasing MWCO of membranes used. Marginal but observable rejection of copper for 6 and 20 KD MWCO membranes indicate that these membranes have pores that are lesser than hydrated ionic diameter of copper ions in solutions.

The solute rejection of PEI even though significantly higher than copper, ranges from 92% for 6 KD and about 70% for 100 KD membranes. This observation also indicates that the fraction of pore diameters of the membrane is higher than the average pore diameter of PEI. The DLS experiments have also indicated the PEI molecular weight is not unique but has molecular weight distribution.

All these observations lead to a conclusion that any behavior of cu–PEI interactions in solutions and their consequent influence in membrane performance depend on the pore-size distribution of the membrane as well as size distribution of PEI.

4.5.1. Experimental observations on the UF membrane performance of Cu in the presence of PEI

Independent experiments were conducted using different weight ratios of Cu/PEI which is referred to as load ratio. PEI concentration is held constant at 160 ppm, while four different Cu concentrations were used, namely 1.6, 16, 63.5, and 160 ppm.

The observed solute rejection of copper in the presence of PEI at fixed concentration is shown in

Table 3
Discretized pore-size distribution of three membranes

Fraction of pores (KD)	0.1	0.1	0.1	0.1	0.1	0.1	0.1	0.1	0.1	0.1
6	0.7	1.5	2.1	2.5	3	3.5	4.0	4.6	5.4	11.0
20	2	2.9	3.5	4.1	4.6	5.1	5.7	6.3	7.2	12.5
100	4.2	5.3	6.0	6.7	7.3	8.0	8.6	9.4	10.5	17.0

Table 4
Weight fraction and the corresponding maximum size of PEI as obtained through DLS measurement

Wt. fraction	0.107	0.281	0.281	0.166	0.089	0.044	0.02	0.008	0.003	0.001
Diameter (nm)	1.8	2.5	3.3	4.5	6.1	8.2	11.1	14.9	20.2	27.2

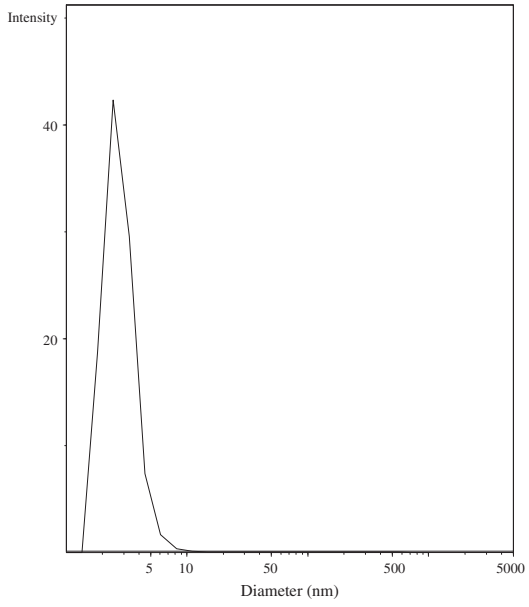

Fig. 6. Size distribution of PEI.

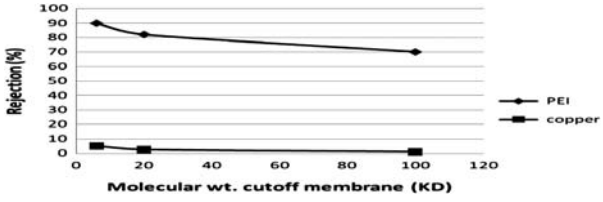

Fig. 7. Rejection of pure PEI (160 ppm) and pure copper (64 ppm) at 2.2 bar pressure.

Fig. 8. As expected, the solute rejection in the entire range of concentrations studied is higher for 6 KD, less for 20 KD, and least for 100 KD. The rejection is almost constant up to about 63.5 ppm of copper (at constant load of 160 ppm of PEI) for all the membranes, and thereafter, there is a decrease in the rejection and the rate of decrease is more for 100 KD less for 20 KD and least for 6 KD.

The maximum solute rejection exhibited by 6 KD membrane is about 94% about 2% higher than the solute rejection exhibited by pure ligand (in the absence of Cu). Similarly, the maximum solute rejections exhibited by 60 and 100 KD membranes are higher compared with pure ligand rejections by about 3.5

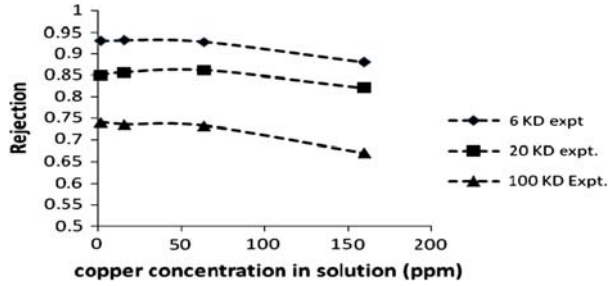

Fig. 8. Solute rejection of copper as a complexed with PEI ligand (160 ppm).

and 4.5%, respectively. These observations clearly indicate that the Cu–PEI complex is larger in size compared with the ligand and hence better rejected.

The rejection behavior of Cu–PEI with increasing ratio of Cu/PEI indicates two distinct regions; one flat zone up to about 63.5 ppm of copper and a drooping zone beyond this concentration for a constant 160 ppm PEI concentration of copper, corresponding to weight ratio of about 0.39 and a molar ratio of 1:3.72 considering unit monomer of PEI ($-(C_2H_5.N)_n-$). This ratio corresponds to 1:n complex of PEI or 1:1 complex of cu and single polymer unit of PEI. The later representation is preferable considering distribution of molecular weight of PEI. Hence, it can be concluded that the flat portion of curve represents the rejection of complexed species. As the Cu concentration is increased beyond this limit, there is no room for complexation, and hence, the rejection starts decreasing or the copper ions permeate through the membranes.

Instead of a sharp fall in solute rejection (which is expected when all excess copper ions permeate through the membrane), the rejection appears to be slowly reducing. The most probable cause could be pore blockage in the membranes due to the presence of complexed species restricting the passage of copper ions. The other possibilities could arise from repulsion of ions [21] and gyration of the ligands [22], which could restrict the permeation of ions.

5. Validation of model

The model equations have been developed by incorporating modifications to the base model (without corrections for poresize distribution and molecular weight distribution for the complex) and later incor-

porating the corrections step by step. At every step, the model performance is compared with field results and the error margin between the experimental values and model values were worked out. The ultimate objective is to minimize the error by incorporating modifications to the base model.

The base model algorithm assumes pure ligand rejection 100% and pure metal rejection 0% as given by Juang chen et al. [3]. Based on this assumption, the model is used to estimate metal rejection R_{Me} with the condition $R_{Mefree} = 0$ and $R_L = 1$ and the error is estimated with respect to experimental values. In next step, mean pore sizes of membrane has been incorporated, and the model performance was compared with the experimental results, and the error was estimated. The second modification involves use of discretized pore sizes of membranes and size distribution of ligand, followed by the estimation of error.

The performance of the base model as seen in Fig. 9 indicates the solute rejection to be independent of Cu concentration as it assumes total ligand rejection and complexing of all the copper with PEI. Further, it is independent of membrane characteristics. The exercise has been done so as to create a base for comparison as the developed model in the current study incorporates the membrane and solute characteristics.

In order to make the model closer to reality, the membrane characteristics in terms of mean pore radii is introduced into the model Eq. (19) for calculating the solute flux (J_s). Further, the mean size of the polymer derived from stoke's radius is introduced into the calculation. The different terms used in Eq. (19) were obtained from Eqs. (11–18). Six sets of q values (three for Cu and three for PEI) were estimated using Eq. (13) corresponding to three membranes and one r_s for Cu and another for PEI. Steric factors (S_D, S_F) and wall correction factors (f, g) of diffusion and filtration flow have been obtained by Eqs. (14)–(17) by utilizing six sets of q values. These factors are incorporated in

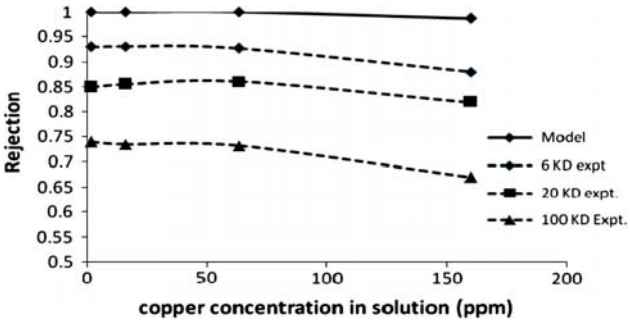

Fig. 9. Performance of base model with experimental results.

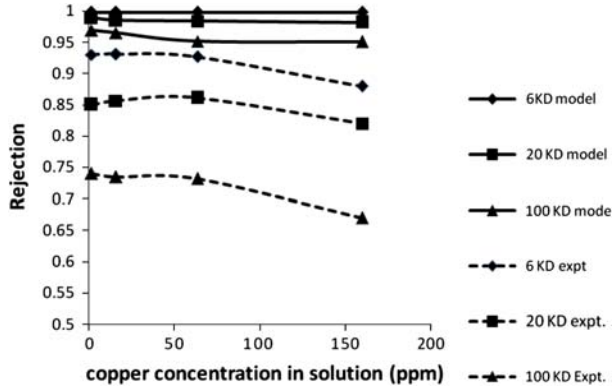

Fig. 10. Validation of experimental rejection data by incorporating mean pore sizes of membranes in mathematical model.

Eqs. (11) and (12) to obtain σ and ω values. From this irreversible model, six sets of product concentration followed by six sets of rejection values have been obtained from Eqs. (19)–(21). Rejection of metal for a particular membrane R_{Me} has been estimated by inserting rejection value of copper in irreversible model Eq. (7). The results obtained from the model for three different membranes are presented along with experimental results in Fig. 10.

The modification has introduced membrane-specific behavior for the Cu–PEI species resulting three different performance curves compared with the base model. The initial portion is in fair agreement but when the Cu concentration is in excess in relation to the complexing potential of PEI the trend itself is different. The error margin has reduced only marginally compared with the base model.

5.1. Validation of experimental rejection data of copper with incorporation of discretized pore sizes of membrane and size distribution of ligand

To further improve the model, it was decided to introduce the pore-size distribution of the membrane and molecular weight distribution of PEI. The calculations were similar to the one carried out earlier except that the metal rejections were carried out for all the weight fractions of PEI (using their maximum size) in combination with each fraction of pore (maximum size) and summing up the rejection. The results are shown in Fig. 11. When the size of particular PEI weight fraction is more than the considered discretized pore size of the membrane, then rejection is taken to be 100%. Otherwise, the rejection is calculated as per the procedure discussed.

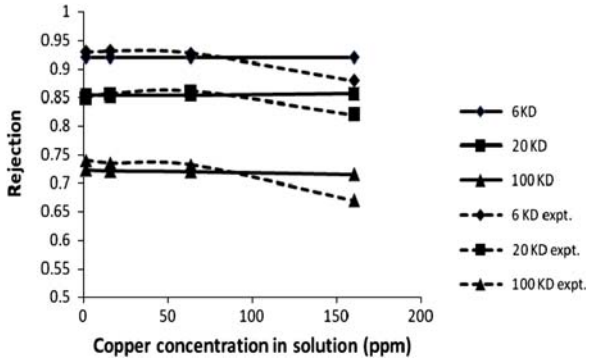

Fig. 11. Validation of experimental metal rejection by incorporating pore-size distribution of membrane and size distribution of polyethylene imine.

The experimental rejection behavior of copper is well predicted by modified mathematical model within the experimental error of measurements (2%). When the copper concentration in solution is higher than what could be complexed by PEI, the model fails to predict even the trend. It is clear from the experimental observations that some factors other than pore size influence the passage of copper through the membranes. The possible reasons could be pore blockage by complexed PEI–Cu species or ionic repulsions between copper ions. In any case, it is not purely a physical phenomenon (related to membrane pore-size or solute size) but requires certain physicochemical phenomenon which warrants separate set of experimental studies. The model is essentially an extension of irreversible thermodynamic model for membrane phenomenon with the expansion of the two coefficients σ, reflecting the membrane nature and ω the size of solute species. Hence, we conclude that the model as developed is good as long as the physical characteristics of the membrane and the solute species control the performance, which is largely true for ultra-filtration membranes. In the case of trace species removal through the membranes, it is expected that the complexing ligand would be in stoichiometrically excess quantities.

The error between the experimental observations and model performances are presented in Table 5. As indicated in the earlier discussions, the error is only around 2% for the model incorporating pore-size distribution of membrane and size distribution of the ligand for the concentrations of copper up to 63.5 ppm, that is, corresponfding to 1:1 complex on single-unit polymer basis. Even though the error is only marginally higher for higher copper concentration and it requires some investigations involving physicochemical aspects, which we have not attempted in this study.

Table 5
Estimated Error between the experimental Values and the model performance

	6 KD			20 KD			100 KD		
Cu Conc. (ppm)	Case-1	Case-2	Case-3	Case-1	Case-2	Case-3	Case-1	Case-2	Case-3
1.6	7.5	7.2	1.0	17.6	16.3	0.56	35.13	30.9	2.3
16	7.4	7.1	1.1	16.8	15.0	0.3	36.05	30.17	1.9
63.54	7.8	7.6	0.7	16.1	14.2	0.8	36.6	30.03	1.6
160	13.6	13.3	4.5	21.9	19.7	4.3	49.2	41.9	6.6

Notes: Case-1 represents pure ligand rejection 100% and pure metal rejection 0% (base model)
Case-2 considers mean pore size of membranes and size of PEI based on average mol.wt.
Case-3 incorporates of discretized pore sizes of membrane and size distribution of ligand.

6. Conclusion

The studies have indicated that the membrane performance is to be analyzed not based on average pore size or average molecular weight of the ligand species. The pore-size distribution and the molecular weight distribution play a major role in the performance of the membrane. Besides, in the presence of complexing ligands, the behavior of excess metal species is not controlled by the pore-size distribution alone but perhaps would involve physicochemical interactions as well.

Nomenclature

A — molecular wt. PEG/PEO;
A_k — ratio of total cross sectional pore area to the effective membrane area;
$(C_s)_{ln}$ — logarithimic solute concentration, kgmole/m^3;
C_m — concentration on membrane surface kgmole/m^3;
C_p — product concentration kgmole/m^3;
D — diffusivity m^2/sec;
$f(q)$ — correction factors for effect of cylindrical walls for filtration flow;
$g(q)$ — correction factors for effect of cylindrical walls for convection flow;
[H] — hydrogen ion concentration kgmole/m^3;
[HL] — concentration of protonated ligand kgmole/m^3;
J_v — solvent flux, m/s;
J_w — pure water permeability, m/s
J_s — solute flux, m/s;
$K_{i,n}$ — equilbrium constant of complex (kgmole/$m^{3)-n}$;
K_a — equilibrium constant of protonated ligand (kgmole/$m^{3)-1}$;
[L] — concentration of ligand in feed (kgmole/$m^{3)}$;
$[L]_{free}$ — concentration of free ligand (kgmole/$m^{3)}$;
L_P — solvent permeability constant M/s.Pa;
[Me] — concentration of metal in feed (kgmole/m^3);
$[MeL_n]$ — concentration of metal ligand complex (kgmole/m^3);
$[Me]_{free}$ — concentration of free metal (kgmole/m^3);
M_w — molecular wt. kg/kgmole;
M — molecular wt. of PEG/PEO kg/kgmole;
n — coordination No.;
N_A — Avogadro's number;
R_L — rejection of ligand;
R_{Me} — rejection of metal;
R_{Mefree} — rejection of free metal;
r_s — solute radius, m;
r_p — pore radius, m;
S_D — steric hindrance factor for diffusive flow;
S_F — steric hindrance factor for filtration flow;
q — ratio of solute radius and pore radius;
$[\eta]$ — specific viscosity, m^3/kg;
ω — solute permeability constant,kgmole/Ns;
μ_p — mean pore size of membranes;
μ — solvent viscosity, Pas
σ — reflection coefficient;
Δp — effective operating pressure, Pa;
ΔX — membrane thickness,m;

References

[1] Baburao S. Mohite, Amol S. Jadhav, Column chromatographic separation of uranium(VI) and other elements using poly (dibenzo-18-crown-6) and ascorbic acid medium, J. Chromatogr. A. 983 (2003) 277–281.
[2] N. Parthasarathy, M. Perlletier, J. Buffle, Permeation liquid membrane for trace metal speciation in natural waters, Transport of liposoluble Cu(II) complexes, J. Chromatogr. A 2004 (1025) 33–40.
[3] R.S. Juang, M.N. Chen, Measurement of Binding Constants of Poly(ethyleneimine) with metal ions and metal chelates in aqueous media by ultrafiltration, Ind. Eng. Chem. Res. 35 (1996) 1935–1943.
[4] Pieter Vonk., Reinoud Noordman, Docke Schippers, Bouke Tilstra, Haus Wesselingh, Ultrafiltration of a polymer-electrolyte mixture, J. Membr. Sci. 130 (1997) 249–263.
[5] Raffel Molinari, S. Gallo, P. Arqurio, Metal-ions removal from wastewater or washing water from contaminated soil by ultrafiltration-complexation, Water Res. 38 (2004) 593–600.
[6] P. Canizares, A. Perez, R. Camarillo, J.J. Linares, A semicontinuous laboratory-scale polymer enhanced ultrafiltration process for the recovery of cadmium and lead from aqueous effluents, J. Membr. Sci. 240 (2004) 197–200.
[7] P. Canizares, A. Perez, R. Camarillo, Maria Teresa Villajos, Improvement and modeling of a batch polyelectrolyte enhanced ultrafiltration process for the recovery of copper, Desalination 184 (2005) 357–366.
[8] P. Canizares, A. Perez, R. Camarillo, J. Llanos, M.L. Lopez, Selective separation of Pb from hard water by a semi-continuous polymer-enhanced ultrafiltration process (PEUF), Desalination 206 (2007) 602–613.
[9] P. Canizares, A. Perez, R. Camarillo, R. Mazarro, Simultaneous recovery of cadmium and lead from aqueous effluents by a semi-continuous laboratory-scale polymer enhanced ultrafiltration process, J. Membr. Sci. 320 (2008) 520–527.
[10] Javier Llanos, A. Perez, Pablo CaniZares, Copper recovery by polymer enhanced ultrafiltration (PEUF) and electrochemical regeneration, J. Membr. Sci. 323 (2008) 28–36.
[11] Javier Llanos, Rafael Camarillo, Angel Perez, Pablo Canizares, Polymer supported ultrafiltration as a technique for selective heavy metal separation and complex formation constants prediction, Sep. Purif. Technol. 73 (2010) 126–134.
[12] S. Singh, K.C. Khulbe, T. Matsura, P. Ramamurthy, Membrane characterization by solute transport and atomic force microscopy, J. Membr. Sci. 142 (1998) 111–127.
[13] Allan S. Michales, Analysis and prediction of sieving curves for ultrafiltration membranes: A universal correlation? Sep. Sci. Technol. 15 (6) (1980) 1305–1322.
[14] Youm Kyung Ho, Kim Woo Sik, Prediction of intrinsic pore properties of ultrafiltration membrane by solute rejection curves: Effects of operating conditions on pore properties, J. Chem. Eng. Japan 24 (1) (1991) 1–7.

[15] E.A. Mason, H.K. Lonsdale, Statistical- mechanical theory of membrane transport, J. Membr. Sci. 51 (1990) 1–81.
[16] T.R. Noordman, J.A. Wesselingh, Transport of large molecules through membranes with narrow pores-The Maxwell-Stefan description combined with hydrodynamic theory, J. Membr. Sci. 210 (2002) 227–243.
[17] Mohamad Soltanieh, William N. Gill, Review of reverse osmosis membranes and transport models, Chem. Eng. Commun.12 (1981) 279–363.
[18] Pappenheimer Jr,. Passage of molecules through capillary wals, Physiol. Rev. 33(3) (1953 Jul) 387–423.
[19] A. Verniory, R. Du Bois, P. Decoodt, J.P. Gassee, P.P. Lambert, Measurement of the permeability of biological membranes—application to the Glomerular Wall, J. Gen. Physiol. 62 (1973) 489–507.
[20] Nakao, Kimura, Analysis of solute rejection in Ultrafiltration, J. Chemical Eng. Japan 14 (1981) 32–37.
[21] Shiro Kobayashi., K. Hioishi, M. Tokunoh, T. Saegusa, Chelating properties of linear and branched polyethyleneimine, Macromolecules 20 (1987) 1496–1500.
[22] Hatsuo Ishida, Properties of Polymers, Department of Macromolecular Science, Western Reserve University, Cleveland, Ohio, 2009.